Machining process simulation using Samcef superelement

Luc MASSET, Jean-François DEBONGNIE
Manufacturing Laboratory, University of Liège, Belgium

Audrey MARTY
Process Engineering Department, Powertrain Division, Renault SAS, France

Abstract: *In this paper, we present a new simulation tool for process engineers. During process design phases, several aspects of machining have to be taken into account. Classical CAD/CAM suites still lack some crucial issues. The goal of the developed tool is to predict the geometric errors of machined surfaces. For classical applications of the automotive domain, form errors are mainly due to the machined part and clamping system flexibility. They are modeled thanks to the FE method. The major peculiarity of the adopted model is to apply numerous load cases. To achieve a low computational cost, we have combined the SAMCEF superelement feature and a specific code to solve the reduced system. This original scheme allows solving efficiently large industrial applications.*

1. Introduction

Nowadays, manufacturing industries demand more and more simulation codes focusing on process issues. Actually, simulation offers the ability to reduce time and costs during process planning phases since less experimental validation is required. Some issues are already well covered by available commercial codes. Let us cite CAD/CAM suites like Catia or Pro-Engineer (NC programming, tool collisions, time cycles …) or specialized software such as CutPro [1] (chatter prediction for end-milling operations). However, huge efforts are to be made to meet all the industrial needs in manufacturing process simulation.

In this aim, we have developed a simulation tool dedicated to *geometric error prediction* such as form or position errors. The purpose is to study the influence of several process parameters (clamping system, tool trajectory, cutting conditions …) on the geometric conformity of the machined surface. In practice, such simulations should allow process engineers to design more rapidly manufacturing operations conforming to the part specifications. In addition, the machinability of the part may be improved by modifying its design according to the simulation results.

Geometric error mechanism is easy to explain. Let us consider the turning operation of a cylindrical bar between centers (figure 1a). If we suppose that the only flexible component of the system is the part (tool, machine-tool and centers are supposed to be rigid), we can model the turning operation as a beam simply supported at both ends and loaded by a radial force *F* moving from one end to the other (figure 1b). A classical analytic formula gives the radial displacements *x(z)* for any tool position (figure 1c). As the part bends under force *F*, the tools leaves a certain amount of material *d(a)* (called the *defect*) on the part surface equal to the opposite of the radial displacement *x(a)* at the tool position. At the end of the turning operation, the machined surface will exhibit a geometric error described by the defects *d(a)* along the bar length (figure 1d).

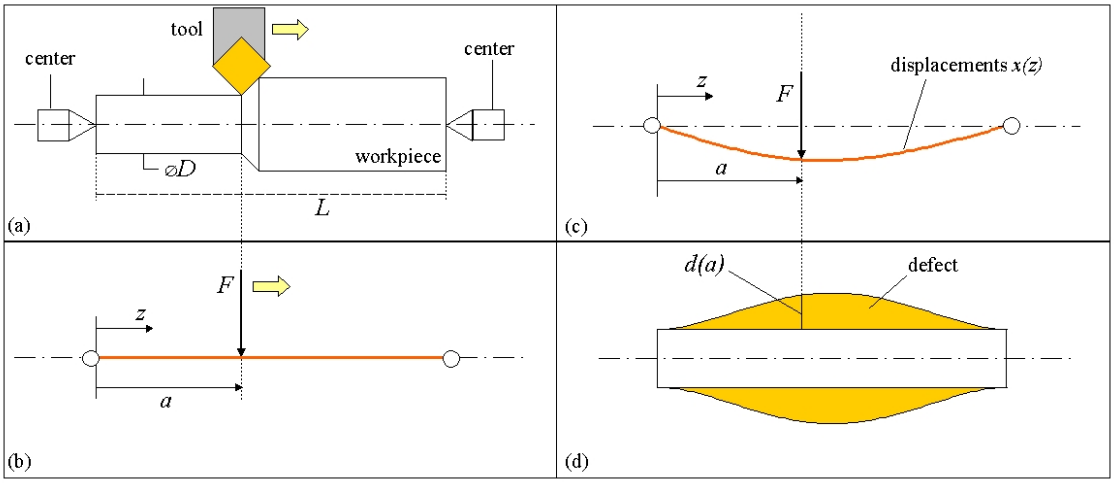

Figure 1: analytical model of a bar turned between centers

2. Finite element approach

For industrial parts, a numerical method such as the finite element method is required to obtain the part deformations occurring along the tool path but the principle remains the same. A few methods are proposed in the literature. Most are based on a time approach, which implies a complex interpolation scheme to obtain the defect of the whole machined surface [2]. We have adopted a method based on a spatial approach: the defect is computed at each node of the machined surface. For each node, we have to:

- compute the tool position and the corresponding cutting forces,
- perform the FE analysis to obtain the whole displacement field,
- extract the displacement of the node and take its opposite to obtain the node defect.

Finally, the defect of the whole machined surface (figure 2) is described by the *n* nodal defects, *n* being the number of nodes on the machined surface [3].

Up to now, we have only worked on applications in the automotive industry for which we can assume tool and machine-tool to be perfectly rigid and for which we have

focused on part and fixture compliance. Therefore the system studied with the finite element method is the part and the clamping devices. In addition, we do not take into account residual stress or thermal aspects which may have a substantial effect in some specific configurations (workpiece made of aluminum castings for example).

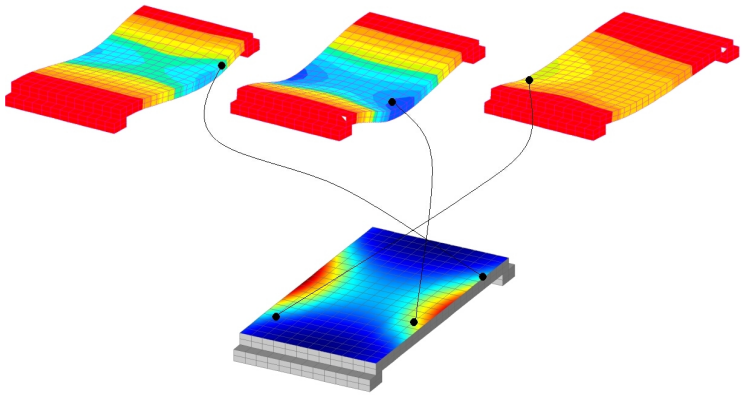

Figure 2: principle of the developed method

From a finite element point of view, the basic concept is simply to solve the equilibrium equations of a system submitted to several load cases, one load case for each node of the machined surface:

$$\boldsymbol{K}\,\boldsymbol{q} = \boldsymbol{g}^{(l)} \qquad l = 1,\ldots,n \tag{1}$$

where $\boldsymbol{K}$ is the stiffness matrix, $\boldsymbol{q}$ are the degrees of freedom and the $\boldsymbol{g}^{(l)}$ are the load vectors. For large industrial applications, the resolution of system (1) is heavily time and memory consuming [4] so that simulation cannot be achieved on standard workstations. The reason is that commercial finite element codes are not designed to solve such problems. So we have developed an original resolution scheme based on the superelement method, available in Samcef code.

3. Resolution scheme

The system to solve presents some specific aspects:

- only displacements need to be computed,
- only a small part of the model dof are involved (boundary conditions or loading),
- only one displacement is required per load case,
- each load case contains numerous zeros.

To take advantage of these peculiarities, we first apply the superelement method. The degrees of freedom of the original system are split into the retained ones, denoted $\boldsymbol{q}_R$, and the condensed ones denoted $\boldsymbol{q}_C$. Original system (1) becomes a smaller one limited only to the retained dof (figure 3). In our case, we chose the retained dof in the

machined surfaces (in blue) and the clamping zones (in orange) as shown in figure 3. One may notice that all terms of $\boldsymbol{g}_C$ are zero since no condensed dof is loaded.

$$\begin{array}{ccc} \boldsymbol{K} & \boldsymbol{q} & \boldsymbol{g} \\ \begin{bmatrix} \boldsymbol{K}_{RR} & \boldsymbol{K}_{RC} \\ \boldsymbol{K}_{CR} & \boldsymbol{K}_{CC} \end{bmatrix} & \cdot \begin{bmatrix} \boldsymbol{q}_R \\ \boldsymbol{q}_C \end{bmatrix} = & \begin{bmatrix} \boldsymbol{g}_R \\ \boldsymbol{0} \end{bmatrix} \end{array}$$

$$\Leftrightarrow \left[\boldsymbol{K}_{RR} - \boldsymbol{K}_{RC}\boldsymbol{K}_{CC}^{-1}\boldsymbol{K}_{CR}\right]\boldsymbol{q}_R = \boldsymbol{g}_R$$

$$\Leftrightarrow \boldsymbol{K}_{RR}^{*}\,\boldsymbol{q}_R = \boldsymbol{g}_R$$

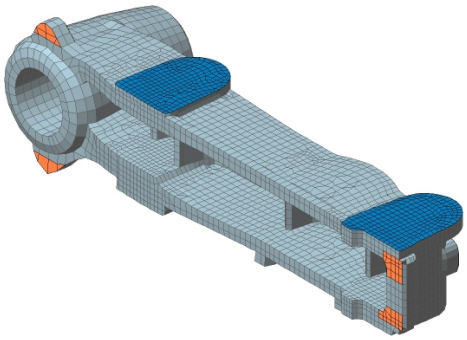

Figure 3: superelement method (left) and superelement for a suspension support (right)

For most applications, the system size is reduced by a factor 50 to 500. In practice, we use Samcef only to create the superelement, in other words, to compute the reduced stiffness matrix $\boldsymbol{K}_{\boldsymbol{RR}}^{*}$. No boundary conditions are set at this stage so this is a pure condensation of the system. Samcef is very efficient for this task thanks to the sparse solver. Table 1 shows the characteristics of the superelement creation for the two applications of figure 4 (machined surfaces are colored in blue and clamping zones in orange).

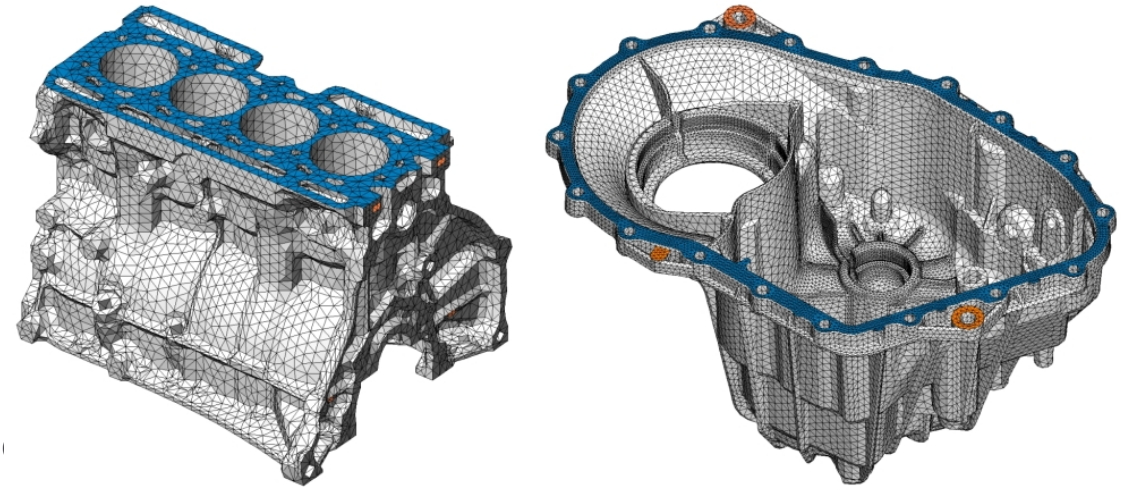

Figure 4: FE models of a 4-cylinders crank case and a gear box case (courtesy of Renault)

	dof	ret. nodes	time (s)	mem (Mb)	disk (Mb)
4-cylinder crank case	329187	859	515	1211	735
gear box case	858054	2664	2605	1197	2367

Table 1: superelement creation phase in Samcef V10.1-02 on a Pentium IV computer with 2Gb of physical memory running Windows XP

The next task is to invert the reduced stiffness matrix $\boldsymbol{K}_{RR}^{*}$ in order to obtain an explicit system

$$\boldsymbol{q}_R = \boldsymbol{S}_{RR}\, \boldsymbol{g}_R^{(l)} \qquad l = 1, \ldots, n \tag{2}$$

where $\boldsymbol{S}_{RR}$ is the flexibility matrix. This task is performed outside the finite element code thanks to an external code. Classical boundary conditions (restrains, springs …) are applied to the stiffness matrix prior to its inversion thanks to a Cholesky algorithm. The time required for this task is given at table 2 for the two applications shown in figure 4. The inversion time no more depends on the original model size but on the superelement size.

	matrix size	time (s)	mem (Mb)
4-cylinder crank case	2577	31	51
gear box case	7539	808	487

Table 2: stiffness matrix inversion

Finally, the explicit system (2) is solved very quickly since we compute only one degree of freedom per load case and we take into account the numerous zeros in the load vectors $\boldsymbol{g}_R^{(l)}$. The time to obtain the solution, including the load vector computation, is the order of ten seconds.

Figure 5 summarizes the three different stages of the resolution scheme. On a single model, one or more superelements are created, depending on the number of machined surfaces. For each superelement, different clamping designs may be studied. Each one requires only the inversion of the superelement stiffness matrix. For each clamping design, several simulations may be performed by varying the process parameters (cutting conditions, tool, trajectory …).

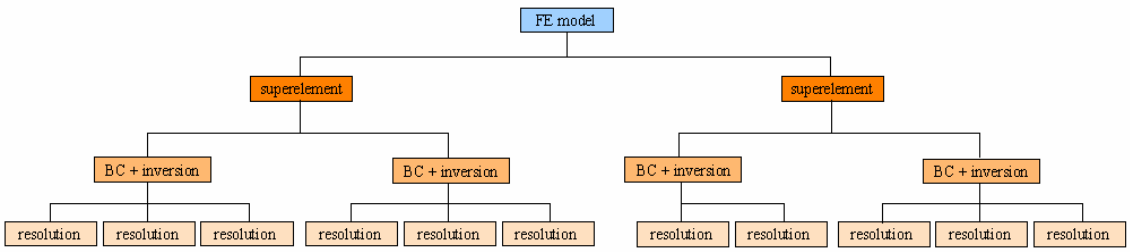

Figure 5: resolution scheme

Thanks to the adopted resolution scheme, the global simulation time for large industrial applications is very small. This renders the developed simulation tool well suited for an industrial use. The software is currently tested in the process planning departments of Renault Powertrain Division (Rueil-Malmaison, Paris) and ACI (Auto Chassis International, Le Mans).

4. Applications

Gear box case

The choice of the clamping zones is usually done according to the experience of the process designers and the geometric constraints imposed by the design department. In most cases, this choice is not optimal. In such situations, simulation may help process designers to find an improved way of clamping a workpiece.

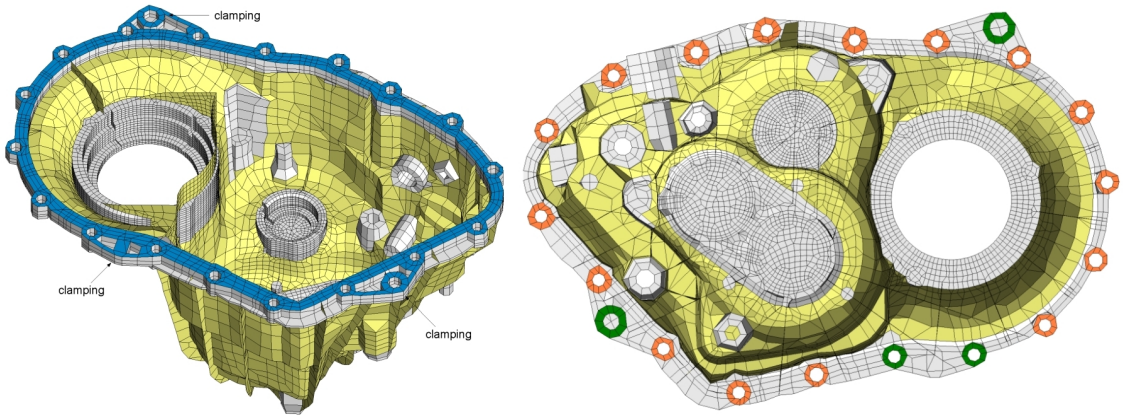

Figure 6: gear box case mesh; 2D elements are coloured in yellow; machined surface in blue; the three original clamping zones are coloured in green while the other possible clamping zones are coloured in orange (courtesy of Renault)

In this application, the part is a gear box case made of aluminum. Figure 6 shows the mesh, composed of both volume elements and 2D elements for the thin walls, and the three original clamping zones. The top surface of the part is face milled. We will use the software to compute the flexibility map of the machined surface for different positions of the clamping zones. First, several possible clamping zones as well as the machined surface are kept in the superelement, so that we are able to change the boundary conditions without creating a new superelement for each set of boundary conditions.

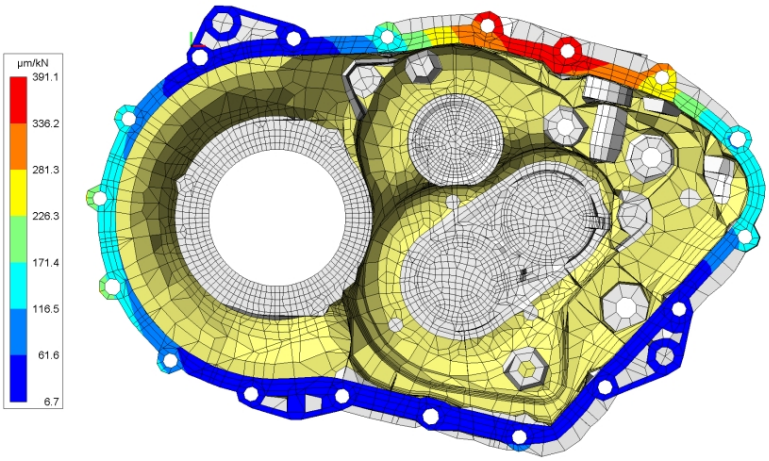

Figure 7: flexibility map of the machined surface for the original clamping design

The flexibility map for the three original clamping zones is shown on figure 7. The part is very flexible outside the triangle formed by the three clamping points (large red zone on the top right). By testing different combinations of three clamping zones, we are able to find the best way to maintain the part. After several trials, we have found a solution (figure 8) where the part flexibility is almost divided by two (stiffness is doubled). This new clamping design is much better than the original one since both geometric defects of the machined surface and risks of vibration (chatter) are lowered.

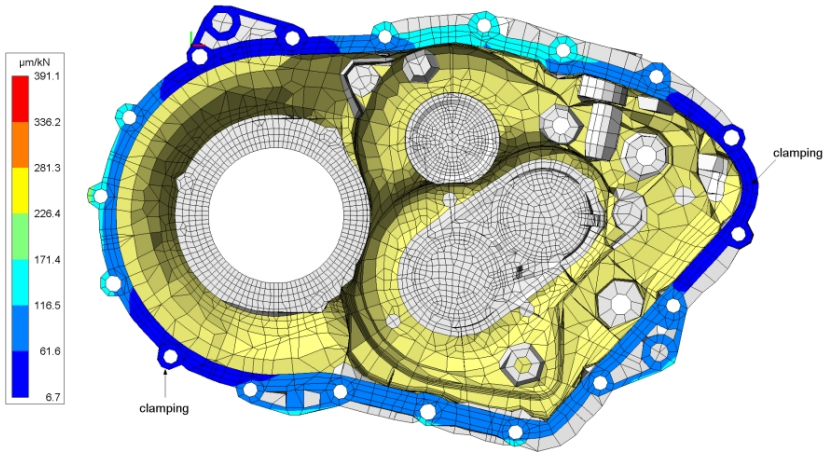

Figure 8: flexibility map for the modified clamping design; two of the three original clamping zones were moved

Brake drum

The part is a brake drum made of cast iron. The clamping system includes three jaws with two contacting zones each and a collar supporting the bottom of the drum (figure 9). The drum is clamped by the radial displacement of the three jaws.

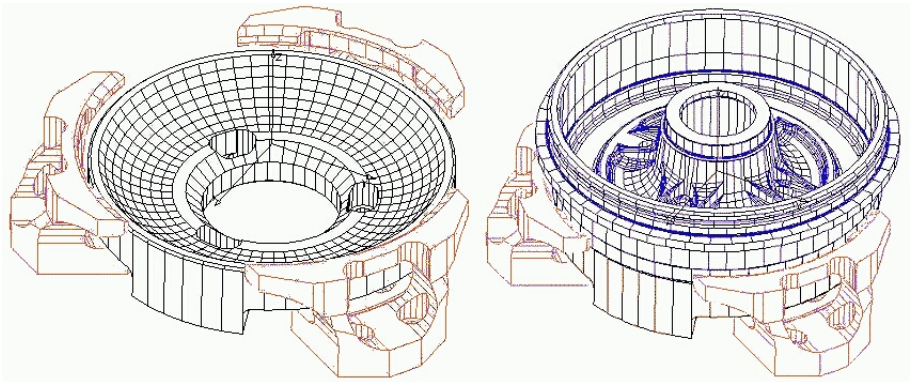

Figure 9: clamping system composed of the three jaws (in red) and the supporting collar (in black); the brake drum is coloured in blue (courtesy of ACI)

The mesh is composed of parabolic tetrahedra. The three jaws were meshed separately from the drum. Thus, we have used Samcef ".stick" elements to glue the different

meshes (figure 10). The supporting collar is modeled with contact conditions on the corresponding nodes of the part.

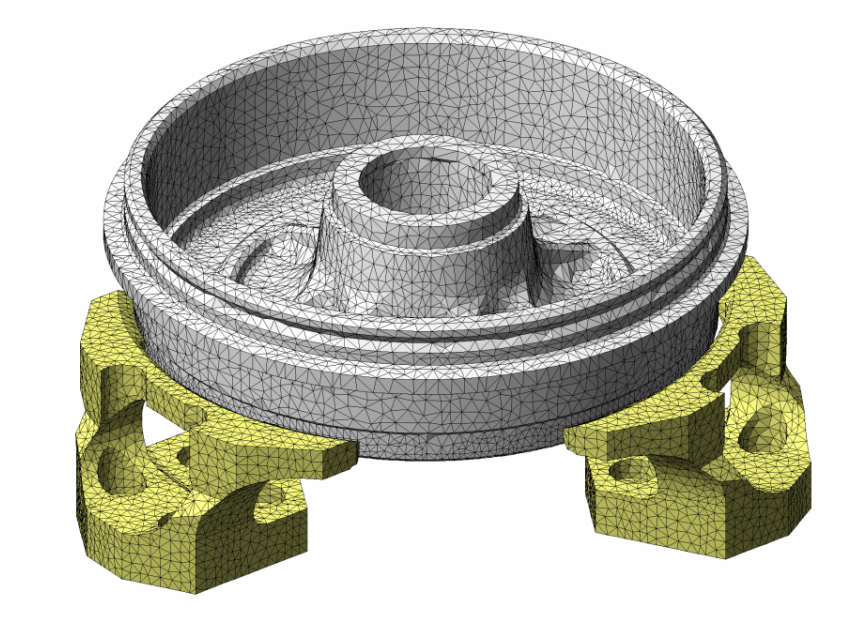

Figure 10: FE model of the drum brake (grey) and the three jaws (yellow)

The machined surface defect obtained by simulation is shown on the left side of figure 11. Checking the displacements of the nodes located on the contacting surface with the collar shows that the part is not in contact with the collar. In fact, the clamping jaws are too flexible to bear the clamping forces: they bend and, consequently, the part does not contact the collar any more.

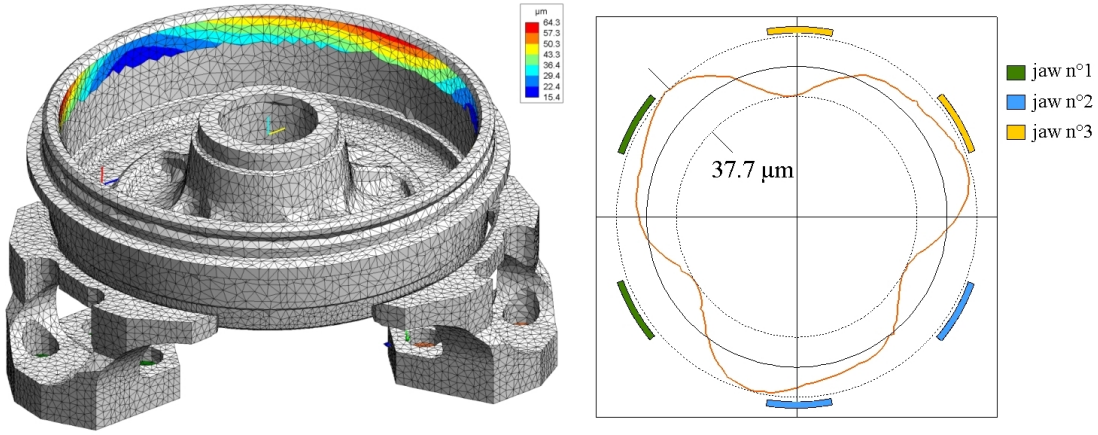

Figure 11: defect of the machined surface (left) and radial run-out curve at the top of the machined surface (right)

The radial run-out curve obtained at the top of the machined surface is shown on the right side of figure 11. The run-out error obtained by simulation equals 37.7 µm while the measured one equals 40 µm. This demonstrates that the developed software gives rather good results when compared to experimental data. For process engineers, the

conclusion to draw from this simulation is that the clamping system is obviously badly designed: the jaws have a huge lever arm (distance between the jaw base and the surface contacting with the drum) only to be able to place the supporting collar; consequently, the jaws bend heavily and lift up the drum so that the collar is of no use. A better design would have been to use stronger jaws without a supporting collar.

5. Conclusion

In the field of manufacturing process simulation, huge efforts have to be made to meet the industry needs. In this aim, the developed software brings new simulation possibilities for process engineers. The peculiarity of process simulation is that many configurations (tool, tool trajectory, clamping design …) have to be tested in order to design valid processes or sequences of operations.

In this work, we have paid a special attention to the computation efficiency. The huge number of load cases is the relevant point of the model. In order to achieve a small computation time, the resolution scheme involves both the superelement method and a specific code. The combination of Samcef power for the superelement creation and the adapted method for solving multi-load case problems allows the resolution of very large industrial applications.

Acknowledgements

We acknowledge Renault (Powertrain Division, Rueil-Malmaison, Paris) and Auto Chassis International (Le Mans) for their technical support.

References

[1] CutPro, Machining Process Simulation Software, www.malinc.com

[2] Gu F., Melkote S. N., Kapoor S. G., Devor R. E., *A Model for the Prediction of Surface Flatness in Face Milling*, ASME Journal of Manufacturing Science and Engineering, vol. 119, pp. 476-484, **1997**

[3] Masset L., *Analyse de gammes d'usinage par la méthode des éléments finis*, PHD thesis, Faculty of Applied Science, University of Liège, Belgium, **2004**

[4] Masset L., Debongnie J.-F., *Machining Process Simulation: Specific Finite Element Aspects*, Journal of Computational and Applied Mathematics, vol. 168, issue 1-2, pp. 309-320, **2004**